Sensors & Actuators: B. Chemical 273 (2018) 635–641

Contents lists available at ScienceDirect

Sensors and Actuators B: Chemical

journal homepage: www.elsevier.com/locate/snb

Nafion-based amperometric H_2S sensor using Pt-Rh/C sensing electrode

Xinyu Yang, Yueying Zhang, Xidong Hao, Yang Song, Xishuang Liang*, Fengmin Liu, Fangmeng Liu, Peng Sun, Yuan Gao, Xu Yan, Geyu Lu*

State Key Laboratory on Integrated Optoelectronics, College of Electronic Science and Engineering, Jilin University, 2699 Qianjin Street, Changchun 130012, China

ARTICLE INFO

Keywords:
H_2S sensor
Nafion
Room-temperature
Fast recovery
Pt-Rh/C Electrode

ABSTRACT

In this paper, an amperometric gas sensor based on proton exchange membrane (Nafion) was fabricated for H_2S detection at room temperature. Pt-Rh nanoparticles loaded on carbon fibers, as sensing electrode, was prepared by chemical reduction method, and membrane electrode assemble (MEA) was fabricated using hot-pressing method. X-ray diffractometry (XRD) and field emission scanning electron microscopy (FESEM) were used to analyze the structure and morphology of the fabricated electrode material. The effect of the weight ratio of Pt to Rh on the performance of the sensor was investigated and the results showed that the sensing performance was best when the ratio of Pt to Rh was 1:1. Moreover, the sensitivity had been significantly improved due to the use of carbon fibers pretreated by nitric acid, increasing from 0.158 μA/ppm to 0.191 μA/ppm. The present sensor could detect H_2S at levels as low as 0.1 ppm with a −20 nA response and had a good linear relationship in the range of 0.1 to 200 ppm H_2S. In addition, this amperometric H_2S sensor displayed fast response-recovery rate as well as excellent selectivity and stability.

1. Introduction

Nowadays, the problem of air pollution has raised more and more attention in various aspects of daily life. The main components of air pollutants are nitrogen oxides (NO_x), carbon monoxide (CO), sulfur dioxide (SO_2), ammonia (NH_3) and hydrogen sulfide (H_2S) [1–10]. Among them, H_2S is one of the most toxic gases and is usually found in sewer, crude petroleum, hot springs and food stuffs [11]. H_2S is colorless, corrosive, flammable and explosive and has a distinctive offensive smell, similar to “rotten egg”, which is a strong neurotoxin that has a strong stimulating effect on mucous membranes. Low concentrations of H_2S can damage the eyes, respiratory system and central nervous system, while inhaled a small amount of high concentrations of H_2S can be fatal in a short period of time [12]. Hence, it is significant to achieve accurate and real-time detection of H_2S.

Currently, the main kinds of H_2S sensors are semiconductor oxide type, electrochemical type and solid electrolyte type. Many studies have been reported on the H_2S sensors based on semiconductor oxides [13–17]. Tong et al. used TiNT (TiO_2 nanotube)-based gas sensor to detect H_2S and attained the response values 4.5–26.2 at 1–50 ppm under the optimum temperature 300 °C [18]. Although these sensors possessed improved properties of gas sensor in certain aspects, high operating temperature, low sensitivity and narrow measurement range still limit their applications. For electrochemical-type sensors, although they can work at room temperature, they usually use a corrosive liquid electrolyte and are easy to dry [19]. For solid electrolyte-type sensors, they usually display good stability and excellent selectivity used yttria-stabilized zirconia (YSZ) and NASICON ($Na_3Zr_2Si_2PO_{12}$) as the electrolytes. Hao et al. reported the YSZ-based mixed potential H_2S sensor using La_2NiO_4 sensing electrode that the sensor performed the highest response of −55 mV to 500 ppb H_2S at an operating temperature of 500 °C [20]. However, these sensors also have the shortcomings such as complex fabrication process and high working temperature. In summary, it is essential to investigate high sensitivity, fast response and wide measurement range gas sensor operating at room temperature.

In the past few years, proton exchange membrane (Nafion) has been used in many fields such as fuel cells, electrolysis cells, flow redox batteries, catalytic and sensor systems due to its good mechanical, outstanding chemical stability and excellent conductivities [21]. The new electrochemical sensor based on Nafion membrane not only has the advantages of zero power consumption, intrinsically safe, environment-friendly, high precision, good stability and long service life, but also can detect trace gases in harsh environments. This sensor has broad application prospects in many fields and can be considered as one of the most important new generation sensors. Recently, many papers have been reported about sensors based on Nafion. Most of the Nafion-based sensors that have been reported are used to detect hydrogen [22,23], carbon monoxide [24,25], oxygen [26,27], while few reports

* Corresponding authors.
E-mail addresses: liangxs@jlu.edu.cn (X. Liang), lugy@jlu.edu.cn (G. Lu).

https://doi.org/10.1016/j.snb.2018.06.087
Received 23 March 2018; Received in revised form 16 June 2018; Accepted 19 June 2018
Available online 20 June 2018
0925-4005/

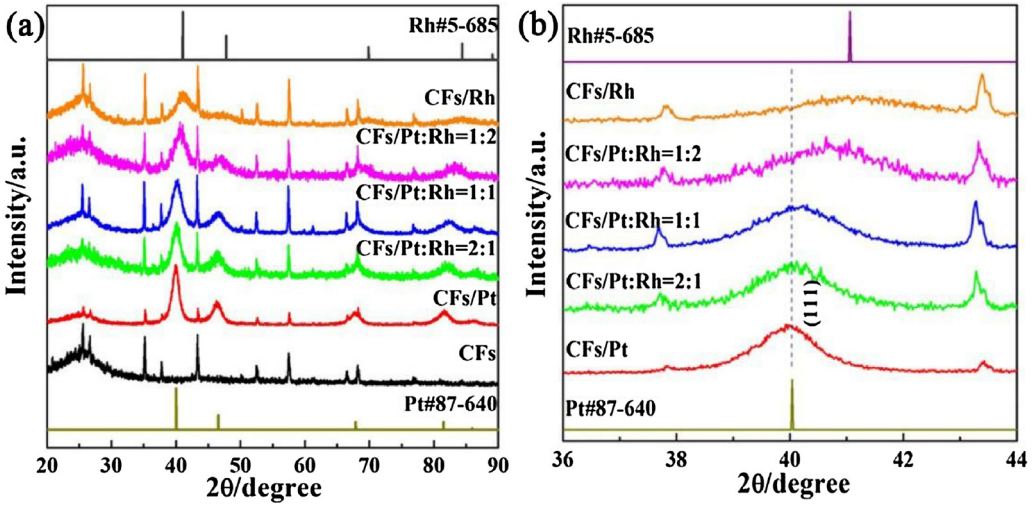

Fig. 1. (a) XRD patterns of five kinds of EMs with different weight ratios of Pt and Rh; (b) Comparison of (111) peaks from XRD patterns.

on the detection of hydrogen sulfide. Therefore, it is very meaningful to develop high-performance Nafion-based H_2S sensor.

In this paper, the platinum (Pt) and rhodium (Rh) nanoparticles deposited on carbon fibers (CFs) are utilized as the composite sensing electrode due to the excellent catalytic properties of this bimetallic catalysts. Effect of loading ratio of Pt and Rh on sensor performance has been discussed. We also pre-treated the CFs with nitric acid to increase the Pt and Rh loadings and thus the sensor response has been significantly improved. During the preparation of the membrane electrode assembly (MEA), we used hot-pressing method to obtain an excellent contact between Nafion membrane and electrode materials (EM) ensuring a good transmission of protons. After that, we assembled the MEA into sensors and investigated the sensing properties as well as mechanism of the Nafion-based amperometric H_2S sensor.

2. Experimental

2.1. Catalyst powder synthesis

Five different sensitive EMs with different weight ratios of Pt and Rh are prepared by chemical reduction method. Total metal loading on CFs was kept consistent at 20 wt.%, wherein the weight ratios of Pt to Rh are 1:0 (EM_a), 2:1 (EM_b), 1:1 (EM_c), 1:2 (EM_d) and 0:1 (EM_e), respectively. Additionally, another kind of EM using CFs ultrasonicated in 68% nitric acid for 4 h at 50 °C is abbreviated to EM_{cp} (Pt:Rh = 1:1). Detailed preparation process is as follows. First, the CF powder is suspended in deionized water with a certain amount of H_2PtCl_6 (Shanghai Wu Chemical Reagent Co., Ltd.) solution and $RhCl_3$ (Shanghai Dibai Chemical Technology Co., Ltd.) in accordance with the above ratios. Then, trisodium citrate ($Na_3C_6H_5O_7{\cdot}2H_2O$, Beijing Chemical Works) is added as the stabilizer at a CF support/trisodium citrate weight ratio of 4:3 by ultrasonication for 30 min. Next, 50 ml reducing agent solution, which is obtained by dissolving the $NaBH_4$ (Aladdin) powders into 50 mL 0.1 M NaOH (Beijing Chemical Works) solution to prevent hydrolysis of $NaBH_4$, is added into the resulting suspension drop by drop. The reaction is carried out under stirring in a water bath at the temperature of 80 °C for 2 h. Finally, the resulting black solid was filtered, washed, and dried at 80 °C for 12 h.

2.2. Fabrication and measurement of the H_2S sensor

The amperometric H_2S sensor is fabricated using the fuel cell prototype containing gas diffusion cap, MEA, isolation disc and water container. Among them, MEA, the core components of this sensor, is produced as follows. 10 mg as-prepared EM powders are well-distributed in 100 μL dispersant which includes 5 wt.% Nafion solution (Shanghai Hesen Electric Co., Ltd.), ethylene glycol (EG, Sinopharm Chemical Reagent Co., Ltd.) and deionized water with the ratio of 2:1:4 on polytetrafluoro-ethylene (PTFE) film. Then two pieces of resulting films are dried at 90 °C and hot-pressed with the Nafion membrane at 90 °C for 90 s. Before this step, in order to remove impurity, the Nafion membranes were pre-treated in 5% H_2O_2 solution (Sinopharm Chemical Reagent Co., Ltd.) for 1 h, 0.5 M H_2SO_4 solution (Sinopharm Chemical Reagent Co., Ltd.) for 1 h and deionized water for 1 h in a water bath at 80 °C, respectively [28]. After that, the PTFE films are peeled away and the MEA is immersed in 0.5 M H_2SO_4 solution for 1 h to replenish lost protons and deionized water for 1 h to remove the sulfuric acid on surface. Here, the H_2S sensors fabricated by above five types of EMs are defined as S_a, S_b, S_c, S_d and S_e, respectively.

X-ray diffraction analysis (XRD, scanning speed: $0.2°s^{-1}$, 2θ ranging from 20°–90°, using CuKα radiation at 0.1541 nm, Rigaku) was used to study the structure, composition, and physical properties of prepared catalyst powders. In order to observe the surface morphology, field emission scanning electron microscopy (FESEM) was used with a JEOL JSM-2100 F microscope operated at an accelerating voltage of 200 kV. In order to study the surface adsorption capacity of different kinds of EMs, the Brunauer–Emmett–Teller (BET) method was used with a Gemini VII surface area and porosity system.

We used chronoamperometry to study the sensitive characteristics of the amperometric H_2S sensor by an electrochemical workstation (CHI611C, Shanghai Instrument Corporation, China). In the process of measurement, the conventional static method was employed by diluting a certain amount of 1% H_2S with air. Moreover, all measurements were carried out under laboratory conditions (23–25 °C, 10–20% RH). The response current (ΔI) is defined as the difference between I_a and I_b, where I_a is the current of sensor in air, I_b is the current in H_2S. We define the time it takes to reach 90% value of ΔI during adsorption and desorption as the response and recovery time of the sensor. The sensitivity is defined as the slope of the liner relationship between ΔI and H_2S concentration.

3. Result and discussion

The XRD patterns of CFs and five kinds of EMs with different weight ratio of Pt and Rh are shown in Fig. 1(a). The XRD patterns show only the five main characteristic peaks of the face-centered cubic (fcc) crystalline structure of Pt and Rh, namely the (111), (200), (220), (311) and (222) planes. For EM_a, five measured peaks are observed at 2θ = 40.0°, 46.4°, 67.9°, 81.6° and 86.3°, which agree well with the Pt cubic structure (JCPDS Card No. 87-640). For EM_e, five measured peaks

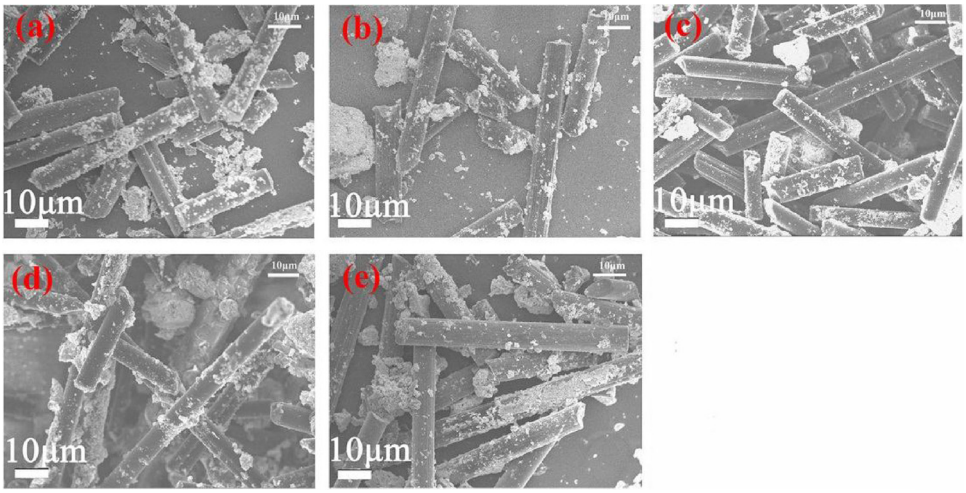

Fig. 2. FESEM images of different weight ratios of Pt and Rh nanoparticles deposited on CFs, (a) CFs/Pt, (b) CFs/Pt:Rh = 2:1, (c) CFs/Pt:Rh = 1:1, (d) CFs/Pt:Rh = 1:2, (e) CFs/Rh.

are observed at 2θ = 41.1°, 47.5°, 70.0°, 84.5° and 89.1°, which agree well with the Rh cubic structure (JCPDS Card No. 5-685). As shown in Fig. 1(b), with the increase of Rh content, slight angle shifts are detected from the (111) peaks. In other words, all the characteristic peaks belong to Pt and Rh, except that the position of these peaks shift to the standard peaks of Rh with the increase in the proportion of Rh. These results showed that Pt and Rh element had been successfully loaded on CFs [29].

The surface morphologies of all the as-prepared EMs are determined as shown in Fig. 2. It can be observed that the Pt and Rh nanoparticles (NPs) are distributed on the surface of CFs. In general, the addition of Rh does not affect the Pt distribution on CFs compared with the results we reported earlier [5]. Due to the smooth surface of CFs, Pt and Rh NPs aggregate in some places and the load is also relatively small. Thus, we pretreated CFs with nitric acid and used them to prepare new EMs. The results of the comparison are given in Fig. 3, which are CFs before (a) and after (b) treatment, electrode materials made from untreated (c) and treated (d) CFs, respectively. Four insets are the enlargement of the above four images. As can be clearly seen from Fig. 3(a) and (b) that CFs pretreated by nitric acid show more potholes than those which are untreated. On the other hand, obviously, it can be found that the Pt and Rh NPs are loaded more and much better distributed on the surface (Fig. 3(c) and (d)). In order to verify the results obtained by SEM, we weighed the EMs prepared with the pre-treated CFs and the untreated CFs (using the same amount of CFs, H_2PtCl_6 and $RhCl_3$). The result shows that the amount of Pt and Rh NPs loaded on CFs after pretreated is 4.8% more than the untreated. Meanwhile, to further confirm the specific surface area and average pore size of these two EMs, the BET nitrogen absorption measurement was applied. It can be seen in Table 1 that the EM_{cp} have a larger BET surface area (9.63 m^2/g) and a smaller

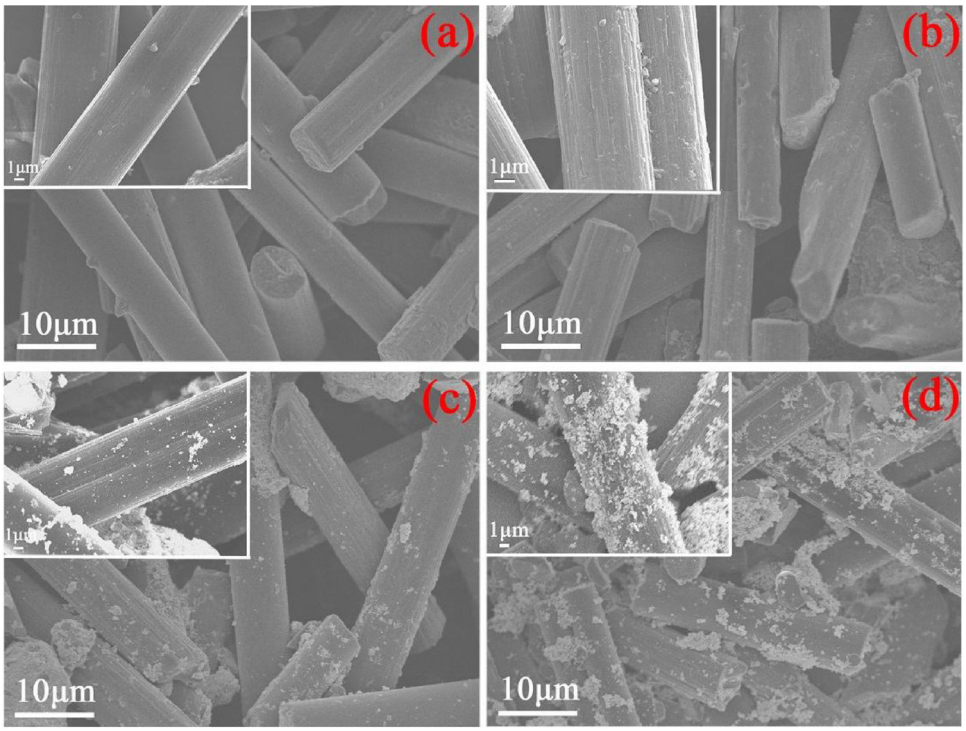

Fig. 3. FESEM images of CFs before (a) and after (b) treatment by 68% nitric acid for 4 h; FESEM images of electrode materials made from untreated (c) and treated (d) CFs.

Table 1
The BET surface areas and average pore diameters of EM_c and EM_{cp}.

Sample	BET Surface Area(m^2/g)	Average Pore Diameter(nm)
EM_c	7.48	20.87
EM_{cp}	9.63	16.05

average pore diameter (16.05 nm), which are 28.74% more and 23.10% less than EM_c. This result also agrees well with the differences shown in the SEM image. Based on the above results, we speculate that the sensor fabricated using EM_{cp} has a better gas sensing performance.

In order to determine the best ratio of Pt and Rh loaded on CFs, firstly, different response current values of 1–50 ppm H_2S for the above five sensors were obtained as shown in Fig. 4(a). It can be seen that the sensitivity of S_a, S_b, S_c are not much different, namely 0.134 μA/ppm, 0.153 μA/ppm and 0.158 μA/ppm. When the ratio of Pt to Rh reaches 1:2, the sensitivity drops to 0.078 μA/ppm drastically. When there is no Pt NP present in the EM, the sensitivity of the sensor is as low as 0.034 μA/ppm, which is shown as S_e in Fig. 4(a). According to M. Farooque and T. Z. Fahidy's works [30,31], the possible oxidation reactions of H_2S (Eqs. (1) and (2)) at the anode side of the MEA are as follows:

$$Pt\text{-}H_2S_{ads.} \rightarrow Pt\text{-}SH_{ads.} + H^+ + e^- \quad (1)$$

$$Pt\text{-}SH_{ads.} \rightarrow Pt\text{-}S_{ads.} + H^+ + e^- \quad (2)$$

The protons generated during the reaction can transfer to the cathode side of the MEA through the Nafion membrane, while, the electrons, can only get to the cathode through the external circuit. Afterwards, the reaction (Eqs. (3) has occurred on the cathode side of the MEA.

$$2H^+ + 1/2O_2 + 2e^- \rightarrow H_2O \quad (3)$$

Therefore, value of the current in the external circuit corresponds to the concentration of H_2S in the gas. For EM_a, EM_b and EM_c, there are abundant active sites for Pt to catalyze the H_2S reaction, thus the sensitivity of S_a, S_b, S_c is very close. And for EM_d and EM_e, the sensitivity becomes very low due to the substantial reduction of active sites. To verify the effect of added Rh on sensor performance, we investigate the selectivity of these five sensors and the result is shown in Fig. 4(b). We can see that as the Rh content increases, the response of sensor to CO decreases significantly. In other words, the addition of Rh effectively suppresses the interference of CO to the sensor. Based on the Nørskov works [32,33], alloying Pt with Rh leads to a down-shift of the Pt 5d-band center caused by the lattice mismatch and the electronic interaction between the Pt and Rh atoms. These phenomena decrease the Pt reactivity or the Pt-CO adsorption strength [34,35]. So, it can be concluded that the addition of Rh can effectively remove the CO on the surface of Pt NPs so that the response of the sensor to H_2S is much larger than the response to CO. Considering the two main factors of sensitivity and selectivity, we ensure that the sensor with Pt to Rh ratio of 1:1 has the best sensing performance. Next, we perform a series of gas-sensing tests on the Pt:Rh = 1:1 sensor (S_{cp}) fabricated using the pretreated CFs.

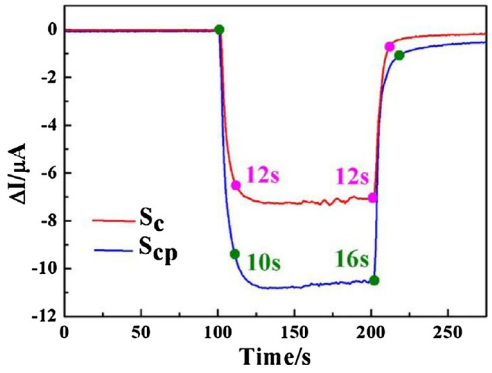

Fig. 5. The typical response transients to 50 ppm H_2S for S_c and S_{cp}.

In order to get the specific impact of pretreatment CFs on the response value, we measured the sensing current of S_c and S_{cp} against 50 ppm H_2S. The sensor was put into H_2S at 100 s and taken out at 200 s. As shown in Fig. 5, S_{cp} shows a larger ΔI value (10.80 μA), 49.2% more than the ΔI value of S_c (7.24 μA). This is mainly because the treated CFs carry more Pt NPs, thus providing more active sites to catalyze the oxidation of H_2S. Similarly, the larger specific surface area will also increase the response current. Moreover, with the increase of the response value, there is no significant increase in the response-recovery time, which is 10 s and 16 s, respectively. This is very fast for H_2S sensors working at room temperature. Such a fast response and recovery time laid the foundation for future sensor applications.

For more information on sensing performance of S_{cp} toward H_2S, the typical response-recovery characteristics to different H_2S concentrations (from 0.1 to 200 ppm) are shown in Fig. 6(a). The sensor was in air and H_2S for 100 s and 150 s, respectively. It is clear that the response current of the sensor increases with the increase of H_2S concentration. The response current can reach a stable platform at low H_2S concentrations (below 100 ppm). The response of S_{cp} to low concentrations of H_2S (0.1, 0.2 and 0.5 ppm) has also been studied as shown in the inset of Fig. 6a. It can be seen that there is an obvious output signal of 20 nA to 0.1 ppm H_2S. In other words, the low detection limit of the sensor is 0.1 ppm. Therefore, this amperometric sensor can detect H_2S in a multi-environment due to its wide range of detection. Moreover, the linear relationships between response currents of S_{cp} and H_2S concentrations in the range of 0.1 to 200 ppm are shown in Fig. 6(b). It

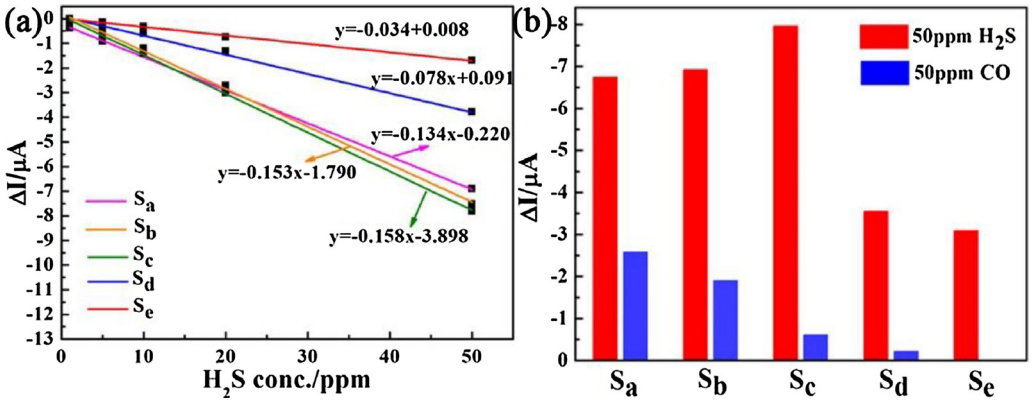

Fig. 4. (a) Sensitivities of sensors to H_2S with different weight ratios of Pt and Rh; (b) Comparison of response values of sensors to CO and H_2S with different weight ratios of Pt and Rh.

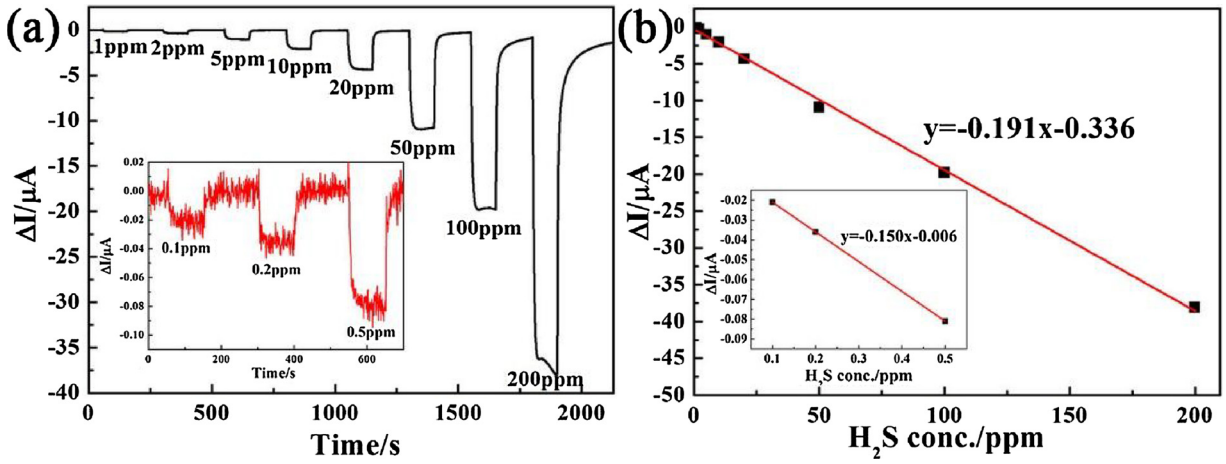

Fig. 6. The typical response transients of S_{cp} to different concentrations H_2S in the range of (a) 1–200 ppm and (b) 0.1-0.5 ppm.

Table 2
Comparison of sensing performances of the present work and that of devices reported in literature.

Sensing electrode	Working temperature (°C)	Recovery time (s)	Low Detection Limit (ppm)	Ref.
Ag-$CaCu_3Ti_4O_{12}$	250°C	850 (10 ppm)	0.2	[36]
Ag-doped α-Fe_2O_3	160°C	35 (50 ppm)	50	[37]
In_2O_3 whiskers	25°C	1200 (20 ppm)	0.2	[38]
CuO thin films	25°C	> 3000 (10 ppm)	0.1	[39]
PPy/WO_3 films	25°C	12,600 (1 ppm)	0.1	[40]
MoO_3/rGO hybrids	110°C	17 (40 ppm)	5	[41]
PI-ZFO	260°C	20 (50 ppm)	1	[42]
SnO_2: NiO thin films	25°C	> 4000 (10 ppm)	0.1	[43]
Co_3O_4 films	200°C	> 50 (40 ppm)	5	[44]
$ZnFe_2O_4$ nanosheets	85°C	34 (5 ppm)	1	[45]
$CoCr_{2-x}Mn_xO4$	250°C	> 500 (10 ppm)	0.1	[46]
Pt-Rh/CFs	25°C	16 (50 ppm)	0.1	This paper

can be seen that these response currents meet a good linear relationship toward different concentrations of H_2S. Additionally, the sensitivity of S_{cp} calculated from the slope of linear relationship between ΔI and H_2S concentrations in the range of 1 to 200 ppm is 0.191 μA/ppm, which is a 20.9% improvement over S_c. From the inset of Fig. 6(b), the sensitivity of S_{cp} was reduced to 0.150 μA/ppm at low concentrations of H_2S (0.1, 0.2 and 0.5 ppm). This is mainly because the consumption of H_2S during the diffusion process has a significant effect on the response of the sensor at low concentrations. Compared with some devices reported in related papers, the present sensor displayed lower working-temperature, lower detection limit and faster recovery rate to H_2S as shown in Table 2.

The continuous response and recovery transients of S_{cp} to 50 ppm H_2S are exhibited in Fig. 7(a). It can be seen that there is not much change in the response current in ten cycles, especially after the first two cycles, the current value is basically unchanged. Therefore, this amperometric H_2S sensor shows an excellent repeatability and can be used for continuous detection.

Selectivity is another important factor in measuring sensor performance. There, different ΔIs of S_{cp} toward 50 ppm of various interference gases (CO, SO_2, NO, NO_2, and NH_3) are shown in Fig. 7(b). Due to the addition of Rh, the response of this sensor to CO is well suppressed. Meanwhile, the response of the sensor to H_2S is also much higher than the response to other gases, which shows an excellent selectivity and has the potential for practical application.

Effect of different relative humidity on response current against

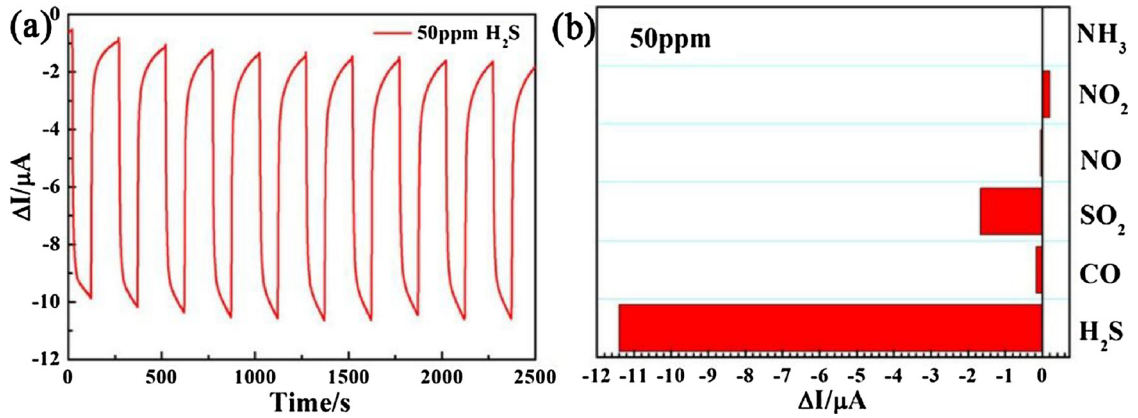

Fig. 7. (a) Continuous response and recovery curves of S_{cp} to 50 ppm H_2S; (b) Cross-sensitivity of S_{cp} to various kinds of gases at a concentration of 50 ppm.

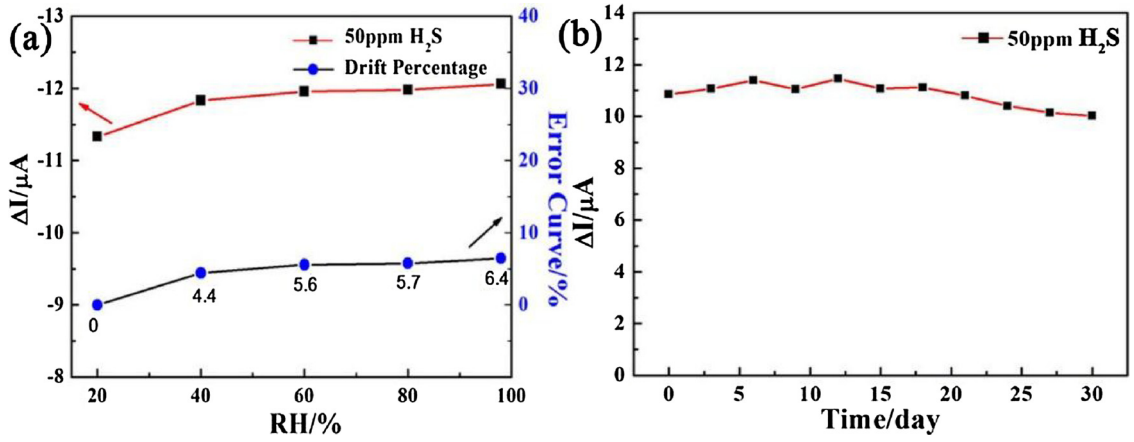

Fig. 8. (a) Response current of S_{cp} toward 50 ppm H_2S at different relative humidity; (b) Long-term stability of S_{cp} toward 50 ppm H_2S.

50 ppm H_2S was measured as shown in Fig. 8(a). As the relative humidity increases, ΔI also increases. We speculate that this is because the conductivity of Nafion membrane strongly depends on the amount of water content. As the relative humidity increases, the conductivity also increases. Here, the drifting percentage is defined as follows: $\Delta I_{error} = (\Delta I - \Delta I_0)/\Delta I_0 \times 100\%$, where ΔI_0 is the sensing current at 20% RH and ΔI is the sensing current at a given RH. It can be seen that when the relative humidity exceeds 60%, the response current of S_{cp} basically no longer changes. The response of the sensor in the test range of 20%–98% RH changed by only 6.4%.

At the end of the work we studied the long-term stability of the sensor. The change of ΔI toward 50 ppm H_2S over 30 days is given in Fig. 8(b). We can see that the response current barely changed in the first 20 days. Although the response current of the sensor decreased slightly after 20 days, it dropped by less than 8%, showing a good stability.

4. Conclusion

In summary, an amperometric H_2S sensor based on Nafion was investigated. We used platinum and rhodium nanoparticles supported on carbon fibers as the sensing electrode material and investigated the effect of different weight ratios of Pt and Rh on sensor performance. The results showed that the sensing performance was best when the ratio of platinum to rhodium was 1:1. We also pretreated carbon fibers by nitric acid and the sensitivity increased from 0.158 μA/ppm to 0.191 μA/ppm. Especially, the recovery time to 50 ppm H_2S was 16 s, which is very fast for H_2S sensors operating at room temperature. Moreover, the low detection limit could reach 0.1 ppm, which had a −20 nA response. In addition, the response current of the sensor in the range of 0.1 to 200 ppm H_2S satisfied a good linear relationship. The sensor also had excellent selectivity and long-term stability. Hence, based on these excellent performance parameters we think this sensor is a promising candidate for application in H_2S monitoring at room temperature.

Acknowledgements

This work was supported by the National Nature Science Foundation of China (Nos. 61473132, 61474057, 61533021 and 61520106003), National Key R&D Program of China (No. 2016YFC0201002) and Program for Chang Jiang Scholars and Innovative Research Team in University (No. IRT-17R47), Application and Basic Research of Jilin Province (20130102010JC), STIRT-JLU (2017TD-07).

References

[1] S. Xu, J. Gao, L. Wang, K. Kan, Y. Xie, P. Shen, L. Li, K. Shi, Role of the heterojunctions in In_2O_3-composite SnO_2 nanorod sensors and their remarkable gas-sensing performance for $NO_{(x)}$ at room temperature, Nanoscale 7 (2015) 14643–14651.
[2] Y. Ge, K. Kan, Y. Yang, L. Zhou, L. Jing, P. Shen, L. Li, K. Shi, Highly mesoporous hierarchical nickel and cobalt double hydroxide composite: fabrication, characterization and ultrafast NO_x gas sensors at room temperature, J. Mater. Chem. A 2 (2014) 4961.
[3] I. Romanytsia, J.-P. Viricelle, P. Vernoux, C. Pijolat, Application of advanced morphology Au-X (X=YSZ, ZrO_2) composites as sensing electrode for solid state mixed-potential exhaust NO_x sensor, Sens. Actuators B Chem. 207 (2015) 391–397.
[4] A. Hosoya, S. Tamura, N. Imanaka, Low-temperature-operative carbon monoxide gas sensor with novel CO oxidizing catalyst, Chem. Lett. 42 (2013) 441–443.
[5] Y. Guan, F. Liu, B. Wang, X. Yang, X. Liang, H. Suo, P. Sun, Y. Sun, J. Ma, J. Zheng, Y. Wang, G. Lu, Highly sensitive amperometric nafion-based CO sensor using Pt/C electrodes with different kinds of carbon materials, Sens. Actuators B Chem. 239 (2017) 696–703.
[6] R. Kumar, D.K. Avasthi, A. Kaur, Fabrication of chemiresistive gas sensors based on multistep reduced graphene oxide for low parts per million monitoring of sulfur dioxide at room temperature, Sens. Actuators B Chem. 242 (2017) 461–468.
[7] Rafael E. de la Hoz, Donald P. Schlueter, William N. Rom, Chronic lung disease secondary to ammonia inhalation injury: a report on three cases, Am. J. Ind. Med. 29 (1996) 209–214.
[8] R.A. Michaels, Emergency planning and the acute toxic potency of inhaled ammonia, Environ. Health Perspect. 107 (1999) 617–627.
[9] K.H. Kim, E.C. Jeon, Y.J. Choi, Y.S. Koo, The emission characteristics and the related malodor intensities of gaseous reduced sulfur compounds (RSC) in a large industrial complex, Atmos. Environ. 40 (2006) 4478–4490.
[10] K.H. Kim, Y.J. Choi, E.C. Jeon, Y. Sunwoo, Characterization of malodorous sulfur compounds in landfill gas, Atmos. Environ. 39 (2005) 1103–1112.
[11] M.Ahmad Khan, Recent trends in electrochemical detection of NH_3, H_2S and NO_x gases, Int. J. Electrochem. Sc. (2017) 1711–1733.
[12] C.R. Csaba Szabo, Katalin Módis, Mireille Andriamihaja, Baptiste Murghes, Ciro Coletta, Gabor Olah, Kazunori Yanagi, Frédéric Bouillaud, Regulation of mitochondrial bioenergetic function by hydrogen sulfide. Part I. Biochemical and physiological mechanisms, Bri. J. Pharmacol. 171 (2014) 2099–2122.
[13] J. Gonzalez-Chavarri, L. Parellada-Monreal, I. Castro-Hurtado, E. Castaño, G.G. Mandayo, ZnO nanoneedles grown on chip for selective NO_2 detection indoors, Sens. Actuators B Chem. 255 (2018) 1244–1253.
[14] X. Kou, N. Xie, F. Chen, T. Wang, L. Guo, C. Wang, Q. Wang, J. Ma, Y. Sun, H. Zhang, G. Lu, Superior acetone gas sensor based on electrospun SnO_2 nanofibers by Rh doping, Sens. Actuators B Chem. 256 (2018) 861–869.
[15] M.N. Rumyantseva, S.A. Vladimirova, N.A. Vorobyeva, I. Giebelhaus, S. Mathur, A.S. Chizhov, N.O. Khmelevsky, A.Y. Aksenenko, V.F. Kozlovsky, O.M. Karakulina, J. Hadermann, A.M. Abakumov, A.M. Gaskov, p-CoO_x/n-SnO_2 nanostructures: New highly selective materials for H_2S detection, Sens. Actuators B Chem. 255 (2018) 564–571.
[16] J. Hu, Y. Liang, Y. Sun, Z. Zhao, M. Zhang, P. Li, W. Zhang, Y. Chen, S. Zhuiykov, Highly sensitive NO_2 detection on ppb level by devices based on Pd-loaded In_2O_3 hierarchical microstructures, Sens. Actuators B Chem. 252 (2017) 116–126.
[17] D. Li, L. Qin, P. Zhao, Y. Zhang, D. Liu, F. Liu, B. Kang, Y. Wang, H. Song, T. Zhang, G. Lu, Preparation and gas-sensing performances of ZnO/CuO rough nanotubular arrays for low-working temperature H_2S detection, Sens. Actuators B Chem. 254 (2018) 834–841.
[18] X. Tong, W. Shen, X. Chen, J.P. Corriou, A fast response and recovery H_2S gas sensor based on free-standing TiO_2 nanotube array films prepared by one-step anodization method, Ceram. Int. 43 (2017) 14200–14209.
[19] B. Spilker, J. Randhahn, H. Grabow, H. Beikirch, P. Jeroschewski, New electrochemical sensor for the detection of hydrogen sulfide and other redox active species, J. Electroanal. Chem. 612 (2008) 121–130.

[20] X. Hao, C. Ma, X. Yang, T. Liu, B. Wang, F. Liu, X. Liang, C. Yang, H. Zhu, G. Lu, YSZ-based mixed potential H_2S sensor using La_2NiO_4 sensing electrode, Sens. Actuators B Chem. 255 (2018) 3033–3039.
[21] E. Safronova, D. Safronov, A. Lysova, A. Parshina, O. Bobreshova, G. Pourcelly, A. Yaroslavtsev, Sensitivity of potentiometric sensors based on nafion®-type membranes and effect of the membranes mechanical, thermal, and hydrothermal treatments on the on their properties, Sens. Actuators B Chem. 240 (2017) 1016–1023.
[22] B.J. Hwang, Y.C. Liu, Y.L. Chen, Characteristics of Pt/nafion® electrodes prepared by a Takenata–Torikai method in sensing hydrogen, Mater. Chem. Phys. 69 (2001) 267–273.
[23] C. Ramesh, N. Murugesan, M.V. Krishnaiah, V. Ganesan, G. Periaswami, Improved nafion-based amperometric sensor for hydrogen in argon, J. Solid State Electrochem. 12 (2007) 1109–1116.
[24] Y. Guan, M. Dai, T. Liu, Y. Liu, F. Liu, X. Liang, H. Suo, P. Sun, G. Lu, Effect of the dispersants on the performance of fuel cell type CO sensor with Pt-C/nafion electrodes, Sens. Actuators B Chem. 230 (2016) 61–69.
[25] K. Mochizuki, A. Yamamoto, T. Kikuchi, M. Sudoh, Y. Gomi, Y. Ishiguro, T. Suzuki, Effects of electrode catalyst loading and membrane degradation for fuel cell type CO sensor, Sens. Lett. 9 (2011) 679–683.
[26] B.J. Hwang, Y.C. Liu, Y.L. Chen, Nafion based solid-state gas sensors: Pt/nafion electrodes prepared by a Takenata-Torikai method in sensing oxygen, J. Chin. Inst. Chem. Eng. 30 (1999) 303–309.
[27] B.J. Hwang, Y.C. Liu, W.C. Hsu, Nafion based solid-state gas sensors: Pd/nafion electrodes prepared by an impregnation-reduction method in sensing oxygen, J. New Mat. Elect. Syst. 2 (1999) 33–38.
[28] K. Furukawa, K. Okajima, M. Sudoh, Structural control and impedance analysis of cathode for direct methanol fuel cell, J. Power Sources 139 (2005) 9–14.
[29] F.H.B. Lima, D. Profeti, W.H. Lizcano-Valbuena, E.A. Ticianelli, E.R. Gonzalez, Carbon-dispersed Pt-Rh nanoparticles for ethanol electro-oxidation. Effect of the crystallite size and of temperature, J. Electroanal. Chem. 617 (2008) 121–129.
[30] T.Z.F.M. Farooque, Low potential oxidation of hydrogen sulfide on a rotating tripolar wiper-blade electrode via continuous anode reactivation, J. Electrochem. Soc. 124 (1977) 1191–1195.
[31] T.Z.F.M. Farooque, The electrochemical oxidation of hydrogen sulfide in the tafel region and under mass transport control, J. Electrochem. Soc. 125 (1978) 544–546.
[32] J. Greeley, J.K. Norskov, M. Mavrikakis, Electronic structure and catalysis on metal surfaces, Annu. Rev. Phys. Chem. 53 (2002) 319–348.
[33] B. Hammer, J.K. Nørskov, Theoretical surface science and catalysis-calculations and concepts, Advances in Catalysis, Academic Press, 2000, pp. 71–129.
[34] F.H.B. Lima, E.R. Gonzalez, Ethanol electro-oxidation on carbon-supported Pt-Ru, Pt-Rh and Pt-Ru-Rh nanoparticles, Electrochim. Acta 53 (2008) 2963–2971.
[35] K. Sasaki, J.X. Wang, M. Balasubramanian, J. McBreen, F. Uribe, R.R. Adzic, Ultra-low platinum content fuel cell anode electrocatalyst with a long-term performance stability, Electrochim. Acta 49 (2004) 3873–3877.
[36] A. Natkaeo, D. Phokharatkul, J.H. Hodak, A. Wisitsoraat, S.K. Hodak, Highly selective sub-10 ppm H_2S gas sensors based on Ag-doped $CaCu_3Ti_4O_{12}$ films, Sens. Actuators B Chem. 260 (2018) 571–580.
[37] Y. Wang, Y. Wang, J. Cao, F. Kong, H. Xia, J. Zhang, B. Zhu, S. Wang, S. Wu, Low-temperature H_2S sensors based on Ag-doped α-Fe_2O_3 nanoparticles, Sens. Actuators B Chem. 131 (2008) 183–189.
[38] M. Kaur, N. Jain, K. Sharma, S. Bhattacharya, M. Roy, A.K. Tyagi, S.K. Gupta, J.V. Yakhmi, Room-temperature H_2S gas sensing at ppb level by single crystal In_2O_3 whiskers, Sens. Actuators B Chem. 133 (2008) 456–461.
[39] N.S. Ramgir, S.K. Ganapathi, M. Kaur, N. Datta, K.P. Muthe, D.K. Aswal, S.K. Gupta, J.V. Yakhmi, Sub-ppm H_2S sensing at room temperature using CuO thin films, Sens. Actuators B Chem. 151 (2010) 90–96.
[40] P.G. Su, Y.T. Peng, Fabrication of a room-temperature H_2S gas sensor based on PPy/WO_3 nanocomposite films by in-situ photopolymerization, Sens. Actuators B Chem. 193 (2014) 637–643.
[41] S. Bai, C. Chen, R. Luo, A. Chen, D. Li, Synthesis of MoO_3/reduced graphene oxide hybrids and mechanism of enhancing H_2S sensing performances, Sens. Actuators B Chem. 216 (2015) 113–120.
[42] J. Wu, D. Gao, T. Sun, J. Bi, Y. Zhao, Z. Ning, G. Fan, Z. Xie, Highly selective gas sensing properties of partially inversed spinel zinc ferrite towards H_2S, Sens. Actuators B Chem. 235 (2016) 258–262.
[43] M. Kaur, B.K. Dadhich, R. Singh, Kailasa Ganapathi, T. Bagwaiya, S. Bhattacharya, A.K. Debnath, K.P. Muthe, S.C. Gadkari, RF sputtered SnO_2 : NiO thin films as sub-ppm H_2S sensor operable at room temperature, Sens. Actuators B Chem. 242 (2017) 389–403.
[44] S.T. Navale, C. Liu, P.S. Gaikar, V.B. Patil, R.U.R. Sagar, B. Du, R.S. Mane, F.J. Stadler, Solution-processed rapid synthesis strategy of Co_3O_4 for the sensitive and selective detection of H_2S, Sens. Actuators B Chem. 245 (2017) 524–532.
[45] X. Gao, Y. Sun, C. Zhu, C. Li, Q. Ouyang, Y. Chen, Highly sensitive and selective H_2S sensor based on porous $ZnFe_2O_4$ nanosheets, Sens. Actuators B Chem. 246 (2017) 662–672.
[46] H. Zhang, T. Zhong, R. Sun, X. Liang, G. Lu, Sub-ppm H_2S sensor based on NASICON and $CoCr_2$-xMn_xO_4 sensing electrode, RSC Adv. 4 (2014) 55334–55340.

Xinyu Yang received the B.Eng. degree in department of electronic science and technology in 2017. He is currently studying for his M.E. Sci. degree in College of Electronic Science and Engineering, Jilin University, China.

Yueying Zhang received the B.Eng. degree in department of electronic science and technology in 2017. She is currently studying for her M.E. Sci. degree in College of Electronic Science and Engineering, Jilin University, China.

Xidong Hao received the B.Eng. degree in department of electronic science and technology in 2016. He is currently studying for his M.E. Sci. degree in College of Electronic Science and Engineering, Jilin University, China.

Yang Song received the B.Eng. degree in department of electronic science and technology in 2017. He is currently studying for his M.E. Sci. degree in College of Electronic Science and Engineering, Jilin University, China.

Xishuang Liang received the B. Eng. degree in Department of Electronic Science and Technology in 2004. He received his Doctor's degree in College of Electronic Science and Engineering at Jilin University in 2009. Now he is a professor of Jilin University, China. His current research is solid electrolyte gas sensor.

Fengmin Liu received the B.E. degree in Department of Electronic Science and Technology in 2000. She received her Doctor's degree in College of Electronic Science and Engineering at Jilin University in 2005. Now she is a professor in Jilin University, China. Her current research is preparation and application of semiconductor oxide, especial in gas sensor and solar cell.

Fangmeng Liu received his Ph.D. degree in 2017 from College of Electronic Science and Engineering, Jilin University, China. Now he is a lecturer of Jilin University, China. His current research interests include the application of functional materials and development of solid state electrolyte gas sensor and flexible device.

Peng Sun received his Ph.D. degree from Jilin University of China in 2014. Now, he is engaged in the synthesis and characterization of the semiconducting functional materials and gas sensors.

Yuan Gao received her PhD degree from Department of Analytical Chemistry at Jilin University in 2012. Now she is an associate professor in Jilin University, China. Her current research is focus on the preparation and application of graphene and semiconductor oxide, especial in gas sensor and biosensor.

Xu Yan received his M.S degree in 2013 from Nanjing Agricultural University. He joined the group of Prof. Xingguang Su at Jilin University and received his Ph.D. degree in June 2017. Since then, he did postdoctoral work with Prof. Geyu Lu. Currently, his research interests mainly focus on the development of the functional nanomaterials for chem/bio sensors.

Geyu Lu received the B.Sci. degree in electronic sciences in 1985 and the M.S.degree in 1988 from Jilin University in China and the Dr. Eng. degree in 1998 from Kyushu University in Japan. Now he is a professor of Jilin University, China. His current research interests include the development of chemical sensors and the application of the function materials.